Journal of Genetics (2023)102:24
https://doi.org/10.1007/s12041-023-01420-2

RESEARCH NOTE

Intronic *OTOF* mutation causes an atypical splicing defect resulting in auditory neuropathy spectrum disorder

SANAZ MOHAMMADI[1], HOSSEIN JAFARI KHAMIRANI[3], SINA ZOGHI[2], SEYED ALIREZA DASTGHEIB[3], SEYED MOHAMMAD BAGHER TABEI[3,4], MAHDIEH TALEBZADEH[5], MOHAMMAD HOSSEIN ADIBI[6] and MEHDI DIANATPOUR[3,7]*

[1]*Comprehensive Medical Genetic Center, Shiraz University of Medical Sciences, Shiraz 71936-13311, Iran*
[2]*Student Research Committee, Shiraz University of Medical Sciences, Shiraz 71936-13311, Iran*
[3]*Department of Medical Genetics, Shiraz University of Medical Sciences, Shiraz 71936-13311, Iran*
[4]*Maternal-fetal Medicine Research Center, Shiraz University of Medical Sciences, Shiraz 71936-13311, Iran*
[5]*Department of Molecular Medicine, Shiraz University of Medical Sciences, Shiraz 71936-13311, Iran*
[6]*School of Biological Sciences, Georgia Institute of Technology, Atlanta, GA 30322, USA*
[7]*Stem Cells Technology Research Center, Shiraz University of Medical Sciences, Shiraz 71936-13311, Iran*
*For correspondence. E-mail: dianatpour@sums.ac.ir.

Received 8 June 2022; revised 27 October 2022; accepted 12 December 2022

Abstract. Pathogenic variants in *OTOF* cause auditory neuropathy spectrum disorder (ANSD), namely prelingual nonsyndromic ANSD and temperature-sensitive ANSD (TS-ANSD). All study subjects provided blood sample for genetic analysis and sequencing. Whole-exome sequencing was carried out to identify the causative pathogenic variant. RNA was extracted to analyse the messenger RNA (mRNA) resulting from the transcription of OTOF. Here, we identified a family with OTOF-related ANSD. This disorder was caused by an intronic mutation in *OTOF* (NM_194248: c.2406+4A>G). In further analysis, we proved that this variant causes a splicing defect resulting in the omission of exon 20 from the mRNA transcribed from *OTOF*. In this study, we demonstrated that the variant is four nucleotides away from the conventional splicing site, and our findings suggest that splicing mechanisms need to be better understood, as well as how neighbouring regions may impact splicing.

Keywords. splicing; splicing defect; OTOF; auditory neuropathy spectrum disorder.

Introduction

Pathogenic variants in *OTOF* cause two distinct types of auditory synaptopathies, namely prelingual nonsyndromic auditory neuropathy spectrum disorder (ANSD) and, a less frequent phenotype, temperature-sensitive auditory neuropathy spectrum disorder (TS-ANSD) (Azaiez *et al.* 2021). Among individuals with ANSD, OTOF is a common genetic cause, responsible for 41–91% of those tested (Zhang *et al.* 2016; Kim *et al.* 2018). OTOF-related ANSD is marked by congenital or prelingual, typically severe-to-profound bilateral hearing loss in the absence of inner-ear anomalies on magnetic resonance imaging (MRI) or computed tomography (CT) imaging of the temporal bones. Otoacoustic emissions (OAEs) are present while auditory brain stem response (ABR) is abnormal at birth. Therefore, newborn hearing screening merely with OAEs will fail to detect this disorder in most patients. OAEs may diminish with age in 20–80% of individuals (Kitao *et al.* 2019).

The hearing loss in ANSD can range from moderate to severe and profound (moderate is defined as hearing loss of 41–55 dB and profound as hearing loss of >90 dB). In some patients, hearing loss may deteriorate throughout early childhood and adolescence (Chiu *et al.* 2010). As is typical of ANSD, individuals with OTOF-related hearing loss have poor speech discrimination, and highly benefit from cochlear implantation. Here, we report a case of OTOF-related ANSD caused by an atypical splicing defect because of an intronic variant located four nucleotides away from the splicing site (NM_194248: c.2406+4A>G).

Published online: 27 February 2023

Materials and methods

Study subjects

All available family members were clinically evaluated for any issues related to the subject of this study. After receiving the informed consents from each individual for participation and publication, we reviewed their medical records. All study subjects provided blood sample for genetic analysis and sequencing. The Ethics Committee of Shiraz University of Medical Sciences approved all of the protocols used for this study.

DNA extraction and sequencing

Using a QIAamp DNA Blood Mini Kit (Qiagen, Hilden, Germany), genomic DNA was extracted from peripheral white blood cells for whole-exome sequencing, Sanger sequencing, and for further investigations. Genomic DNA was captured using the SureSelect XT Human All Exon V6 reagent kit (cat. no. 5190-8863; Agilent Technologies), which was applied for the enrichment of codinfeg exons and flanking intronic sequences in accordance with the manufacturer's instructions. Captured coding DNA samples were sequenced using an Illumina NovaSeq6000 (Illumina San Diego, USA) with 100-bp paired-end sequencing. The raw data were aligned against the human reference genome (hg19) using the Burrows–Wheeler aligner (Li and Durbin 2010). By using Genome Analysis Toolkit, single-nucleotide polymorphisms (SNPs) were identified. Variants were annotated using ANNOVAR (Wang *et al.* 2010). Each variant was classified into one of five categories, namely pathogenic, likely pathogenic, variant of unknown significance (VUS), likely benign, and benign, based on the ACMG standards for the interpretation of sequence variations (Richards *et al.* 2015). The phenotypic features associated with the candidate genes were compared with the patient's phenotype. Core phenotypes of the variants were obtained from the OMIM database and utilized to acquire a gene list for a virtual panel using the OMIM database (OMIM: 601071).

We confirmed the presence of the variants by Sanger sequencing (figure 1b). The primers were designed using Oligo Primer Designer (Rychlik 2007).

RNA extraction and cDNA synthesis

RNA was isolated from sorted cell populations using QIAamp RNA Blood Mini Kit (Qiagen, Hilden, Germany) and treated with RNase-free DNase I (SinaClon, Tehran, Iran) as per manufacturer's instructions. RNA concentration and purity were evaluated by NanoDrop spectrophotometer (ND-1000, Wilmington, USA). One microgram of DNA-free RNA was used for synthesis of cDNA by reverse transcription using AddScript cDNA Synthesis Kit (Addbio, Korea) according to the manufacturer's instructions. Reverse transcriptase was inactivated by incubation at 70°C for 10 min. The cDNAs were stored at −20°C until use. PCR using four primers (table 1) were utilized to analyse the cDNA and presence or absence of exon 20.

All methods were carried out in accordance with relevant guidelines and regulations. This study was ethically approved by Ethics Committee of Shiraz University of Medical Sciences. Written informed consent was provided by the participants or their legal guardian/next of kin to participate in this study. In case of participants under the age of 18, the written informed consent for publication of clinical details and/or clinical images was obtained from their legal guardian/next of kin.

Results

The proband (V-1) is a 36-year-old female born to healthy consanguineous parents (figure 1a). She was diagnosed with profound (> 95 dB) hearing loss by audiometry at 6 months of age. She completed her education until high school diploma.

Her aunt (IV-3) is a 72-year-old female also born to healthy consanguineous parents. She started taking metformin for type II diabetes and amlodipine for hypertension since the age of 55 and 57, respectively. At infancy, her parents noted that she had hearing issues; however, she did not receive medical care until adulthood. She was also diagnosed with profound (> 95 dB) hearing loss by audiometry. Both had work-ups resembling sensorineural hearing loss including negative auditory brainstem response, absent middle acoustic ear muscle reflexes, and bowl-shaped audiogram.

Whole-exome sequencing in individual V-1 identified a variant in *OTOF* (NM_194248: c.2406+4A>G). Sanger sequencing confirmed the presence of mentioned variant in homozygous form. Moreover, the same mutation was found in individual IV-1 in a homozygous form. Individuals IV-2, IV-3, and V-2 were also heterozygous for the aforementioned variant.

Both patients use sign language for their communications and are married. The patients were otherwise healthy and did not have any other significant health issues.

Mutation analysis

PCR conducted using primers 1 and 2 on the affected individuals showed that exon 20 was omitted from their mRNA. Further sequencing showed that the exon sequence detected in other family members is intact (figure 2).

PCR utilizing primers 2 and 3 in the patients resulted in a 335 bp band while in other individuals resulted in two bands, 335-bp and 426-bp long, indicating the deletion of exon 20

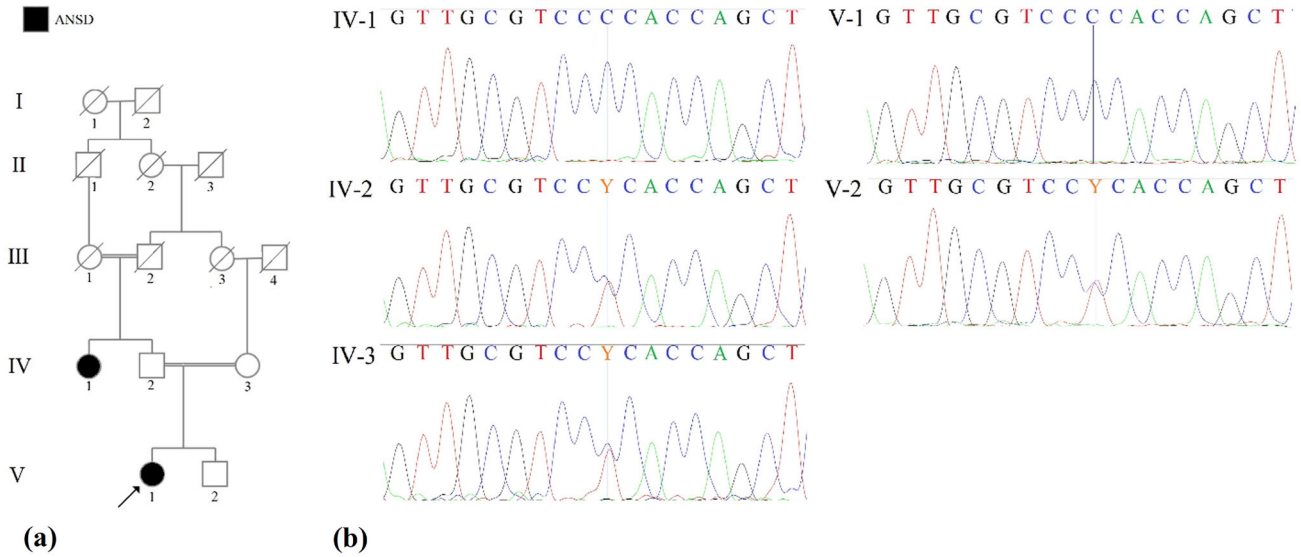

Figure 1. Pedigree and electropherogram of the ANSD patients. (a) Pedigree; (b) electropherogram of the proband (V-1), her aunt (IV-1), her father (IV-2) and her mother (IV-3).

Table 1. The primers utilized in this study for analysis of the effect of the mutation on the mRNA transcribed from *OTOF*. Primer 4 was used to control DNA contamination of the cDNA samples (which was negative).

	Exon	Sequence
Primer 1	Forward 20	TGATCAAAACGGAGAAGTC
Primer 2	Reverse 22	CCACTCATCCCGCACCAG
Primer 3	Forward 19	AGAGCGTCTTGACCTTGG
Primer 4	Forward 19 prime	CCACACTCCTGATTCACA

in the affected individuals. Further sequencing showed that exon 20 is absent from the amplified regions of the affected individuals. PCR utilizing primers 2 and 4, targeting intronic regions, failed to come up with any significant band, which showed that contamination with DNA was not present (figure 2).

The variant discovered in his study is registered at ClinVar (The variant is available under SCV002500937at ClinVar).

Discussion

Here, we report the association of an autosomal recessive ANSD with an intronic mutation in *OTOF* (NM_194248: c.2406+4A>G). Introns are spliced out from the primary transcripts by cleavage at conserved sequences called splice sites. The mentioned sites are located at 5′ and 3′ ends of introns. Typically, the removed RNA sequence begins with a GU dinucleotide at the 5′ end, and ends with AG dinucleotide at its 3′ end (Clancy 2008). Splice-site defects are typically caused by mutations in the aforementioned nucleotides. In this study, we report a novel mutation, four nucleotides away from the 5′ end of the intron 20 of *OTOF*.

Clinical investigations on two members of a family suggested that this mutation, when homozygous, can cause ANSP resembling the patients with OTOF-related ANSD reported previously. To confirm the pathogenicity of the variant and the mechanism underlying the defect in OTOF, we carried out reverse transcription polymerase chain reaction (RT-PCR). RT-PCR showed that the mRNA transcript form *OTOF* containing the variant lacked exon 20, causing a major defect in the structure of OTOF, which subsequently lead to phenotype of the affected family members. The results indicate that c.2406+4A is among the conserved sequences required for splicing.

Splice site defects are common among the variants leading to genetic disorders. These defects are essentially caused by the alterations in the sequence of the first few nucleotides in the 5′ and 3′ ends of introns. To our surprise, we discovered that the variant reported here, four nucleotides away from the 5′ end of the intron 20, which is not paradigmatically listed in the nucleotides involved in mRNA splicing, caused inappropriate splicing of the mRNA and ensuing deficiency in the protein.

There is no experimentally obtained structure of OTOF containing the exon 20. Moreover, there is no evidence available on the exact function of exon 20. As a result, it is difficult to attribute any function to it and make conclusions about its effect on the function of the protein apart from structural integrity of the protein. Figure 3 illustrates the predicted three dimensional structure of OTOF and the location of residues translated from exon 20 on it (figure 3).

This study further proves that on top of the classic nucleotides responsible for intron splicing, nonclassical nucleotides can also be involved in this process and should be considered in the diagnosis of genetic diseases as

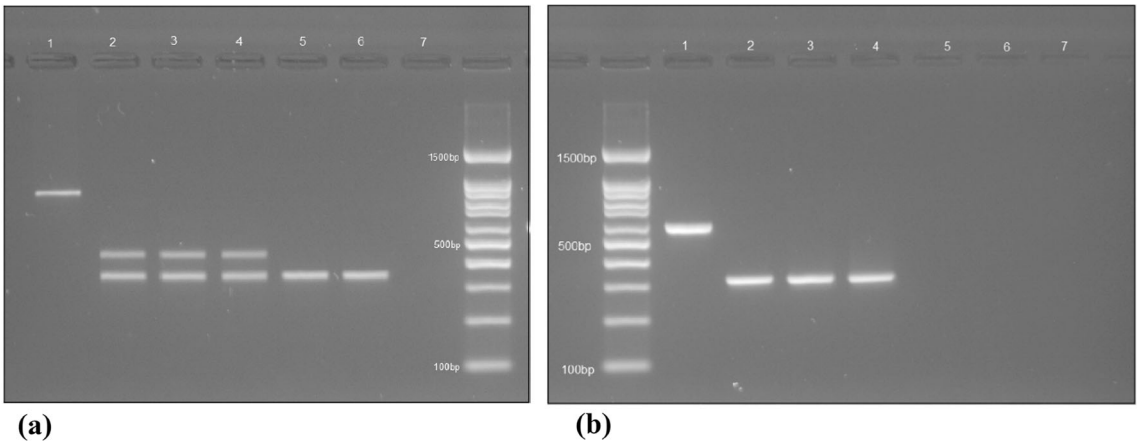

Figure 2. Gel electrophoresis of the PCR products. (a) utilizing primers 2 and 3 from table 1; (1) PCR amplification of DNA sample (including both exon- and intron-coding regions). (2, 3, and 4) PCR products of the cDNA obtained from IV-2, IV-3, and V-2, respectively showing two bands (335 and 426 bp, respectively) depicting the absence of the cDNA corresponding to the exon 20 in one of the alleles. (5 and 6) PCR products of the cDNA obtained from IV-1 and V-1 showing a single 335-bp long band indicating omission of exon 20 from both alleles. (7) The negative control. (b) Utilizing primers 1 and 3 from table 1, PCR amplification of DNA sample using a primer targeting a sequence within exon 20. (2, 3, and 4) PCR products of the cDNA obtained from IV-2, IV-3, and V-2, respectively showing a single 320-bp long band depicting the presence of the cDNA corresponding to the exon 20. (5 and 6) PCR products of the cDNA obtained from IV-1 and V-1 failing to form any band indicating total absence of exon 20 from both alleles. (7) Negative control.

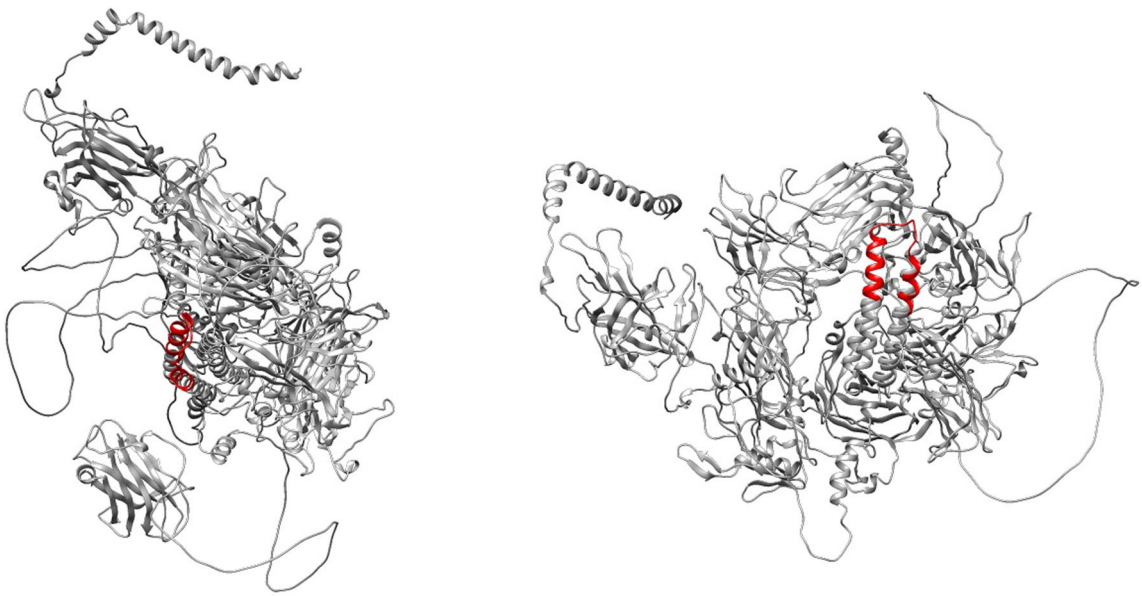

Figure 3. Three-dimensional structure of OTOF and the location of the residues translated from exon 20 on it based on AlphaFold structure prediction (Jumper *et al.* 2021).

illustrated here. The findings of the current study and the previous studies suggest that not only the alterations in the intronic nucleotides are classically regarded as splice sites but also the neighbouring variants, as far as the four nucleotides are away from the exon–intron junction (table 2). Almost all of the studies summarized in table 2 identified exon skipping as the culprit for pathogenicity of these variant. Nevertheless, Khan *et al.* (2020) emphasized that the exon skipping effects several noncanonical splice site variants associated with inherited diseases may be corrected by other splice site of the affected exon and exon inclusion is strongly reliant on the combined strengths of its 5′ and 3′ splice sites. These observations show that our understanding of this phenomenon is severely inadequate and we need a better grasp of the exon–intron junction, splicing, and the way the splicing sites are recognized in cells. As a result, further studies on the prevalence of such variants, their potential applications in molecular genetics and biotechnology, and implications in clinical genetics are highly solicited.

Table 2. A review of previously reported disease-causing variants located four nucleotides away from the splice sites reported in the literature.

Variant	Gene	Associated disease/phenotype MIM number	ACMG pathogenicity category	References
NM_001040142.2: c.3972+4A>G	*SCN2A*	1. Developmental and epileptic encephalopathy 11 613721 2. Episodic ataxia, type 9 618924 3. Seizures, benign familial infantile, 3 607745	Uncertain significance	Lord *et al.* (2019)
NM_001032221.3: c.325+4A>G	*STXBP1*	Developmental and epileptic encephalopathy 4 612164	Uncertain significance	Lord *et al.* (2019)
NM_000350.3: c.302+4A>C	*ABCA4*	1. Cone–rod dystrophy 3 604116 2. Fundus flavimaculatus 248200 3. Retinal dystrophy, early-onset severe 248200 4. Retinitis pigmentosa 19 601718 5. Stargardt disease 1 248200 6. {Macular degeneration, age-related, 2} 153800	Pathogenic	Khan *et al.* (2020)
NM_004006.3: c.1812+4T>A	*DMD*	1. Becker muscular dystrophy 300376 2. Cardiomyopathy, dilated, 3B302045 3. Duchenne muscular dystrophy 310200	Uncertain significance	Khan *et al.* (2020)
NM_138691.3: c.362+4T>A	*TMC1*	1. Deafness, autosomal dominant 36 606705 2. Deafness, autosomal recessive 7 600974	Uncertain significance	Khan *et al.* (2020)
NM_001040667: c.1327+4A>G	*HSF4*	Cataract 5, multiple types 116800	Uncertain significance/likely pathogenic	(Smaoui *et al.* 2004)
NM_005529.7: c.8464+4A>G	*HSPG2*	1. Dyssegmental dysplasia, Silverman–Handmaker type 224410 2. Schwartz–Jampel syndrome, type 1 255800	Uncertain significance/likely pathogenic	Nicole *et al.* (2000)

Table 2 (*contd*)

Variant	Gene	Associated disease/phenotypeMIM number	ACMG pathogenicity category	References
NM_005529.7: c.7294+4A>G	*HSPG2*	1. Dyssegmental dysplasia, Silverman–Handmaker type 224410 2. Schwartz–Jampel syndrome, type 1 255800	Uncertain significance/likely pathogenic	Nicole *et al.* (2000)
NM_014946.4: c.1245+4A>G	*SPAST*	Spastic paraplegia 4, autosomal dominant 182601	Pathogenic	Svenson *et al.* (2001)
NM_000051.4: c.3153+4A>G	*ATM*	1. Ataxia-telangiectasia 208900	Likely pathogenic	Bonache *et al.* (2018)
NM_025137.4: c.1456+4A>C	*SPG11*	1. Amyotrophic lateral sclerosis 5, juvenile 602099 2. Charcot–Marie–Tooth disease, axonal, type 2X 616668 3. Spastic paraplegia 11, autosomal recessive 604360	Likely pathogenic	Zhang (1998); Buratti *et al.* (2007)
NM_000051.4: c.8151+4A>T	*ATM*	1. Ataxia-telangiectasia 208900 2. Breast cancer, susceptibility to 114480	Likely pathogenic	Zhang (1998); Buratti *et al.* (2007)
NM_000302.4(): c.741+4G>C	*PLOD1*	Ehlers–Danlos syndrome, kyphoscoliotic type, 1 225400	Likely benign	Zhang (1998); Buratti *et al.* (2007)
NM_005026.5: c.2055+4A>G	*PIK3CD*	1. Immunodeficiency 14A, autosomal dominant 615513 2. Immunodeficiency 14B, autosomal recessive 619281	Likely pathogenic	Zhang (1998); Buratti *et al.* (2007)
NM_004565.3: c.585+4C>A	*PEX14*	Peroxisome biogenesis disorder 13A (Zellweger) 614887	Uncertain significance	Zhang (1998); Buratti *et al.* (2007)
NM_004958.4: c.3654+4A>G	*MTOR*	1. Focal cortical dysplasia, type II, somatic 607341 2- Smith–Kingsmore syndrome 616638	Likely pathogenic	Zhang (1998); Buratti *et al.* (2007)

Acknowledgement

This study was financially supported by Shiraz University of Medical Sciences.

Authors' contributions

Conceptualization: HJK, SM, and MD; investigation: SM, SAD, MT, and SMBT; supervision: SAD, SMBT, and MD; writing original draft: MHA and SZ; writing review and editing: SZ All authors reviewed and agreed to the final version of the manuscript.

References

Azaiez H., Thorpe R. K. and Smith R. J. H. 2021 OTOF-related deafness. *GeneReviews*. University of Washington, Seattle; 1993–2022.

Bonache S., Esteban I., Moles-Fernández A., Tenés A., Duran-Lozano L., Montalban G. *et al*. 2018 Multigene panel testing beyond BRCA1/2 in breast/ovarian cancer Spanish families and clinical actionability of findings. *J. Cancer Res. Clin. Oncol.* **144**, 2495–2513.

Buratti E., Chivers M., Královičová J., Romano M., Baralle M., Krainer A. R. *et al*. 2007 Aberrant 5′ splice sites in human disease genes: mutation pattern, nucleotide structure and comparison of computational tools that predict their utilization. *Nucleic Acids Res.* **35**, 4250–4263.

Chiu Y.-H., Wu C.-C., Lu Y.-C., Chen P.-J., Lee W.-Y., Liu A.Y.-Z. *et al*. 2010 Mutations in the OTOF gene in Taiwanese patients with auditory neuropathy. *Audiol. Neurotol.* **15**, 364–374.

Clancy S. 2008 RNA splicing: introns, exons and spliceosome. *Nat. Educ.* **1**, 31.

Jumper J., Evans R., Pritzel A., Green T., Figurnov M., Ronneberger O. *et al*. 2021 Highly accurate protein structure prediction with AlphaFold. *Nature* **596**, 583–589.

Khan M., Cornelis S., Sangermano R., Post I. J. M., Groesbeek A. J., Amsu J. *et al*. 2020 In or out? New insights on exon recognition through splice-site interdependency. *Int. J. Mol. Sci.* **21**, 2300.

Kim B. J., Jang J. H., Han J. H., Park H.-R., Oh D. Y., Lee S. *et al*. 2018 Mutational and phenotypic spectrum of OTOF-related auditory neuropathy in Koreans: eliciting reciprocal interaction between bench and clinics. *J. Transl. Med.* **16**, 330.

Kitao K., Mutai H., Namba K., Morimoto N., Nakano A., Arimoto Y. *et al*. 2019 Deterioration in distortion product otoacoustic emissions in auditory neuropathy patients with distinct clinical and genetic backgrounds. *Ear. Hear.* **40**, 184–191.

Li H. and Durbin R. 2010 Fast and accurate long-read alignment with Burrows-Wheeler transform. *Bioinformatics.* **26**, 589–595.

Lord J., Gallone G., Short P. J., McRae J. F., Ironfield H., Wynn E. H. *et al*. 2019 Pathogenicity and selective constraint on variation near splice sites. *Genome Res.* **29**, 159–170.

Nicole S., Davoine C.-S., Topaloglu H., Cattolico L., Barral D., Beighton P. *et al*. 2000 Perlecan, the major proteoglycan of basement membranes, is altered in patients with Schwartz-Jampel syndrome (chondrodystrophic myotonia). *Nat. Genet.* **26**, 480–483.

Richards S., Aziz N., Bale S., Bick D., Das S., Gastier-Foster J. *et al*. 2015 Standards and guidelines for the interpretation of sequence variants: a joint consensus recommendation of the American College of Medical Genetics and Genomics and the Association for Molecular Pathology. *Genet. Med.* **17**, 405–423.

Rychlik W. 2007 OLIGO 7 primer analysis software. *Methods Mol. Biol.* **402**, 35–60.

Smaoui N., Beltaief O., BenHamed S., M'Rad R., Maazoul F., Ouertani A. *et al*. 2004 A homozygous splice mutation in the HSF4 gene is associated with an autosomal recessive congenital cataract. *Invest. Ophthalmol. vis. Sci.* **45**, 2716–2721.

Svenson I. K., Ashley-Koch A. E., Gaskell P. C., Riney T. J., Cumming W. J., Kingston H. M. *et al*. 2001 Identification and expression analysis of spastin gene mutations in hereditary spastic paraplegia. *Am. J. Hum. Genet.* **68(1)**, 077–1085.

Wang K., Li M. and Hakonarson H. 2010 ANNOVAR: functional annotation of genetic variants from high-throughput sequencing data. *Nucleic Acids Res.* **38**, e164.

Zhang M. Q. 1998 Statistical features of human exons and their flanking regions. *Hum. Mol. Genet.* **7**, 919–932.

Zhang Q.-J., Han B., Lan L., Zong L., Shi W., Wang H.-Y. *et al*. 2016 High frequency of OTOF mutations in Chinese infants with congenital auditory neuropathy spectrum disorder. *Clin. Genet.* **90**, 238–246.

Corresponding editor: Ashwin Dalal